Article

Thermal Management of Solar Photovoltaic Cell by Using Single Walled Carbon Nanotube (SWCNT)/Water: Numerical Simulation and Sensitivity Analysis

Mohsen Sharifpur [1,2], Mohammad Hossein Ahmadi [3,*], Jaroon Rungamornrat [4,*] and Fatimah Malek Mohsen [5]

1 Department of Mechanical and Aeronautical Engineering, University of Pretoria, Pretoria 0002, South Africa
2 Department of Medical Research, China Medical University Hospital, China Medical University, Taichung 404, Taiwan
3 Faculty of Mechanical Engineering, Shahrood University of Technology, Shahrood 3619995161, Iran
4 Center of Excellence in Applied Mechanics and Structures, Department of Civil Engineering, Faculty of Engineering, Chulalongkorn University, Bangkok 10330, Thailand
5 Air Conditioning and Refrigeration Department, AL-Mustaqbal University College, Hillah 51001, Babylon, Iraq
* Correspondence: mohammadhosein.ahmadi@gmail.com (M.H.A.); jaroon.r@chula.ac.th (J.R.)

Abstract: Despite the attractiveness of Photovoltaic (PV) cells for electrification and supplying power in term of environmental criteria and fuel saving, their efficiency is relatively low and is further decreased by temperature increment, as a consequence of absorption of solar radiation. In order to prevent efficiency degradation of solar cells due to temperature increment, thermal management is suggested. Active cooling of solar cells with use of liquid flow is one of the most conventional techniques used in recent years. By use of nanofluids with improved thermophysical properties, the efficiency of this cooling approach is improvable. In this article, Single Walled Carbon Nano Tube (SWCNT)/water nanofluid is used for cooling of a PV cell by considering variations in different factors such as volume fraction of solid phase, solar radiation, ambient temperature and mass flow rate. According to the findings, use of the nanofluid can lead to improvement in performance enhancement; however, this is not significant compared with water. In cases using water and the nanofluid at 0.5% and 1% concentrations, the maximum improvement in the efficiency of the cell compared with the cell without cooing were 49.2%, 49.3 and 49.4%, respectively. In addition, sensitivity analysis was performed on the performance enhancement of the cell and it was noticed that solar radiation has the highest impact on the performance enhancement by using the applied cooling technique, followed by ambient temperature, mass flow rate of the coolants and concentration of the nanofluid, respectively. Moreover, exergy analysis is implemented on the system and it is noticed that lower ambient temperature and solar radiation are preferred in term of exergy efficiency.

Keywords: nanofluid; solar energy; PV cell; thermal management; sensitivity analysis

1. Introduction

In regard to fossil fuel sources' limitations, fluctuation in their cost and environmental pollution, cleaner energy technologies using renewable energy sources such as wind and solar have been developed in recent decades [1–3]. The solar photovoltaic (PV) cell is one of the most fascination technologies used for clean power generation [4]. The attractiveness of PV cells is mostly attributed to the possibility of power generation in different scales, simple operation and installation, relatively low maintenance cost and availability of solar radiation in different regions. Due to these advantages of solar cells, these systems are applied for different purposes, including electrification of buildings in remote areas and supplying the power to different systems such as desalination plants,

electrolyzers, etc. [5–8]. Despite the advantages, relatively low efficiency in addition to the unavailability of solar radiation in night hours, meaning no power generation, are the main disadvantages. In order to overcome the problem related to unavailability of solar power during night hours, using storage units such as batteries is recommended. In terms of resolving the issues concerning low efficiency, several methods and solutions have been proposed including the modification of cell material, use of concentrators and providing the operating conditions leading to performance enhancement [9,10]. Numerous elements including solar radiation, operating conditions, working temperature, material of the cell, etc., influence the operation and output of solar cells [11–13]. One of the most influential operating factors that influences the cell efficiency is temperature. Increment in the temperature of PV cells degrades their efficiency and consequently the output at constant solar radiation. In this regard, thermal management of cells is recommended to achieve better efficiency without any change in the operating elements.

Performance of thermal management applied in PV cells, influencing the cell temperature and output power, depends on certain elements. Conventional approaches applied for cell thermal management are divided into two main groups: active and passive [14]. In active methods, such as making use of fluid flow for heat removal from the cell, an additional component such as a pump or fan is used to circulate a fluid in order to cool down the cell, while in passive methods, such as Phase Change Material (PCM), there is no additional energy consuming unit [15–17]. Using PCM and heat pipes without activity in the condenser section are some of the passive approaches that are used for thermal management of cells [16,18]. These techniques have shown significant performance in decreasing the temperature of cells and consequently improving efficiency and output [19]. In spite of the acceptable performance of passive techniques, using active methods can be preferred in term of heat transfer. Temperature reduction of cells in cases using active methods depends on various elements. In active methods with coolant flow, using liquids is preferred due to their higher heat transfer capacity compared with gases. Use of liquids for cooling the cell remarkably decreases the temperature of the cell and improves its efficiency. For instance, Shalaby et al. [20] found that using water cooling for a PV cell can causes around 14% increase in power generation. Regarding the influence of the thermal properties of the liquids in heat transfer of fluid flows, use of liquids with modified properties, e.g., nanofluids, would be more beneficial for efficient thermal management. In some studies [21], both active and passive methods such as PCM and liquid flow have been integrated in order to arrive at a technique with higher efficiency in cooling the cell. Despite the better performance of these approaches, based on the integration of two or more techniques, the complexity of the system is increased.

Nanofluids are prepared by the dispersion of solid materials with nanometer dimensions in a base fluid. The solid phase can be in different shapes, such as cylinder, platelet, tubes, etc. Dispersion of the solid phase in the base fluid leads to modification in some thermal properties such as thermal conductivity [22,23]. Variations in the properties of the fluids regarding the existence of the solid phase is affected by different elements such as the material of solids, concentration, features of the fluid, etc. [24,25]. Generally, addition of solid phase will increase thermal conductivity and dynamic viscosity, while the specific heat is mainly decreased due to the lower specific heat of solid materials compared to the liquids used as base fluids. In the following section, equations are provided which are used for the estimation of these properties. Regarding the increment in thermal conductivity, convective heat transfer of nanofluids can be higher compared with conventional fluids without solid nanoparticles. The modified characteristics of nanofluids, in term of heat transfer, make them an attainable alternative to the conventional fluids used for thermal management and heat transfer [26]. Nanofluids have been extensively used in different solar systems in recent years [27]. Making use of nanofluids in the solar system would improve the overall performance. For instance, Nazari et al. [28] used Fe_3O_4/Ag hybrid ferro particles in the basin water of a solar still and observed an increment in the productivity of the systems. In another study [29], Cu_2O nanoparticles were applied in a solar

still integrated with a thermoelectric cooling channel. Making use of the nanofluid with 0.08% concentration caused 81% improvement in the productivity of the system. In another work [30], Cu_2O nanoparticles were used in a solar water heating system, based on an evacuated tube solar collector and concentrator, and improvement in exergy efficiency of the system was around 12.7%.

Thus far, regarding the significant effect of active approaches in thermal management, several studies have focused on this concept; however, some aspects have not been considered. In this study, Single Walled Carbon Nanotube (SWCNT)/water nanofluid, as one of the most conductive nanofluids, is applied as coolant for thermal management of a cell in order to boost heat transfer as much as possible. In order for full investigation, several factors such as concentration of nanofluid, mass flow rate, solar radiation and ambient temperature are taken into consideration and their effects are discussed. Furthermore, exergy analysis is implemented to obtain a better insight into the system. Finally, sensitivity analysis is carried out in order to determine the importance level of various factors. In the following sections, methodology, results and conclusion are provided.

2. Material and Methods

To numerically investigate the effect of various cooling parameters on performance, a PV cell, monocrystalline silicon type, is considered, with length and width of 200 mm and 83 mm, respectively. Five layers, glass, EVA, cell, EVA and Tedlar, are considered in the module as shown in Figure 1. The thicknesses of these layers are 3 mm, 0.5 mm, 0.5 mm, 0.5 mm and 1 mm, respectively. In addition, a cooling channel with length and width of 3 mm is used for cooling the cell. In order to show the simulation procedure, applied equations and assumptions are represented in this section.
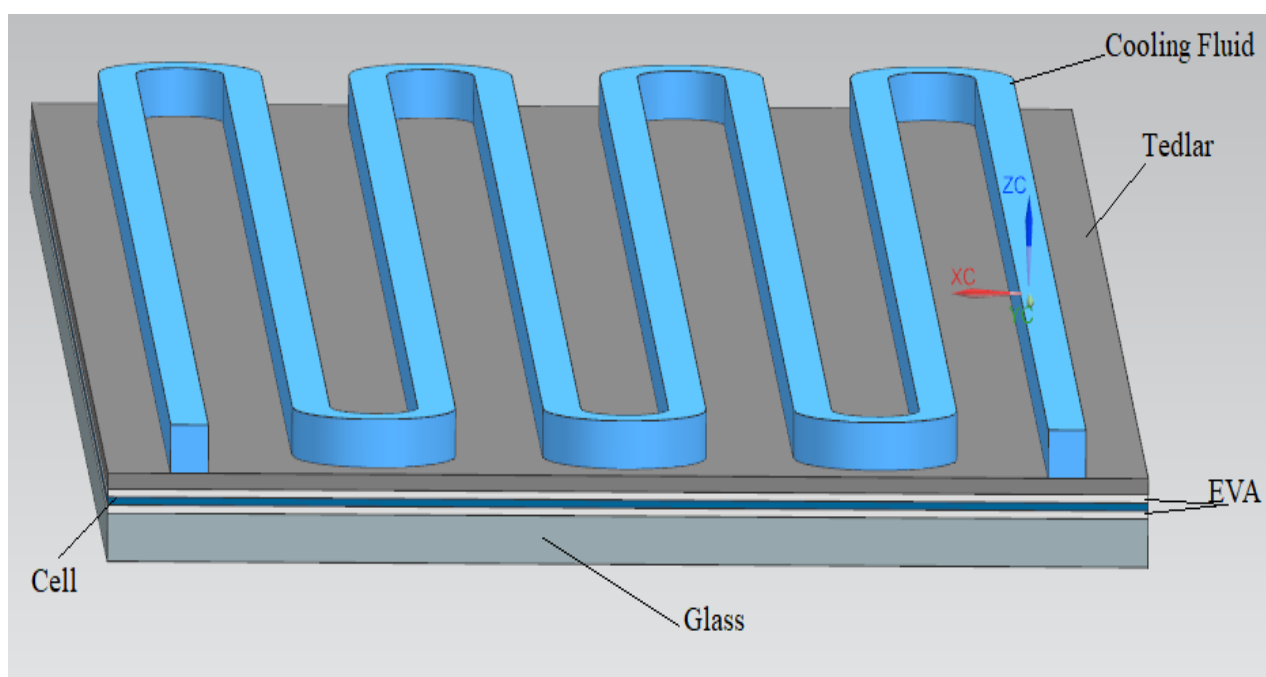
Figure 1. Schematic of the PV module and its sublayers.

For numerical simulation and determination of the cell temperature and efficiency, an energy equation is applied. According to Figure 2, absorbed energy from solar radiation is partly converted into electrical energy. The remaining part causes increment in the internal energy of the cell, dissipated via radiation or convection from the walls. For simplification of the simulation, produced electricity is considered as heat dissipation by considering the variations of efficiency with temperature of the cell.
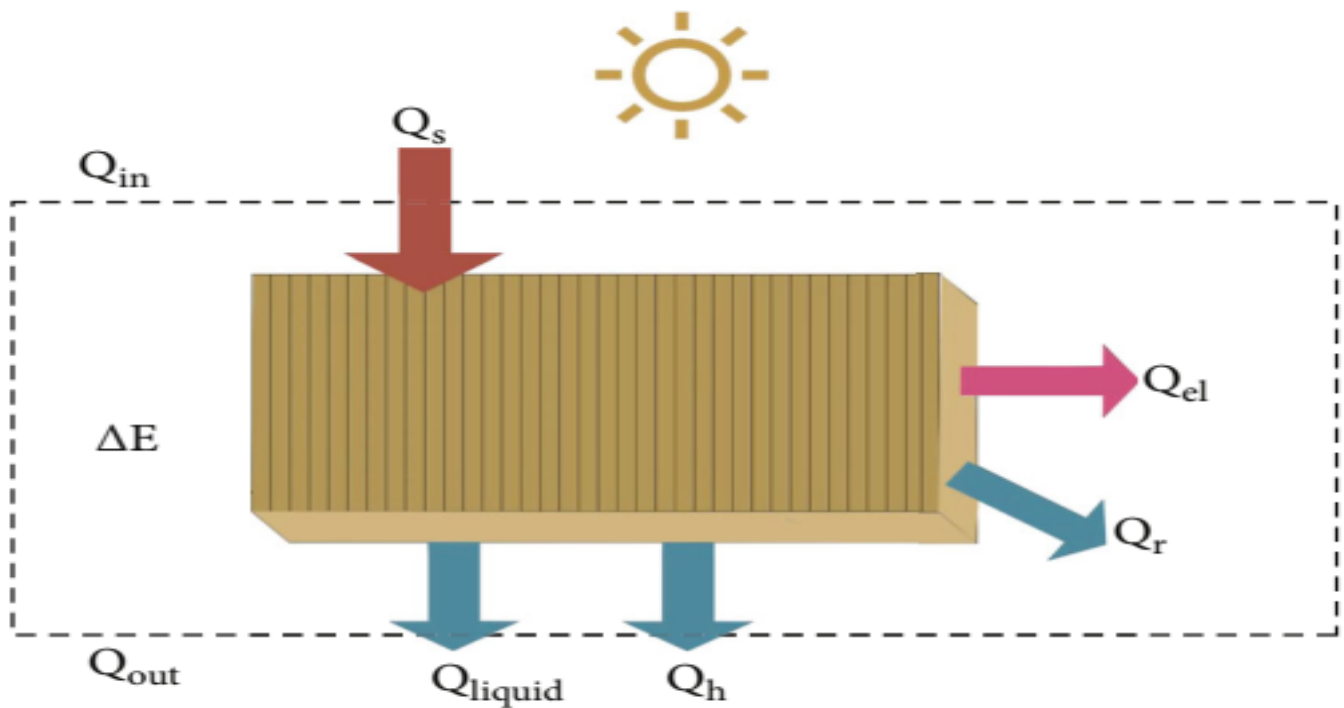
Figure 2. Solar panel energy conservation [31].

Energy conversion in solar cell can be given by Equation (1):

$$\rho C_p \delta \frac{dT_s}{dt} = q_s - q_{el} - q_h - q_r - q_{liquid} \tag{1}$$

where q_s, q_{el}, q_h, q_r and q_{liquid} are absorbed heat from solar radiation by the cell, generated electricity, heat transfer due to convection, heat transfer due to radiation and heat removal by the liquid flow, respectively. Absorbed heat from solar radiation is calculated by using Equation (2) as follows:

$$q_s = \varepsilon_0 Q_s \tag{2}$$

where Q_s and ε_0 are normal solar radiation and absorption coefficient, assumed as equal to 0.9, respectively. Electricity generation by the cell is dependent on efficiency and is determined as follows:

$$q_{el} = \beta Q_s \tag{3}$$

where β is the temperature-dependent efficiency of the cell and is calculated as follows [32]:

$$\beta = -0.1757\, T_s + 21.737 \tag{4}$$

In Equation (4), T_s denotes the cell temperature. Other heat transfer terms related to convection and radiation are determined as follows [32]:

$$q_h = h_h\, (T_s - T_a) \tag{5}$$

$$q_r = \varepsilon_1 \sigma_{sb} \left(T_s^4 - T_a^4 \right) \tag{6}$$

where T_a and h_h are ambient temperature and coefficient of convection heat transfer, respectively. σ_{sb} and ε_1 are Stefan Boltzmann constant and emissivity of cell, respectively. In Equation (5), T_a and h_h are ambient temperature and convective heat transfer coefficient, respectively. In Equation (6), ε_1 and σ_{sb} are emissivity and Stefan Boltzmann constant $(5.67 \times 10^{-8}\ \frac{W}{m^2 K^4})$, respectively. Radiative heat transfer is applied on both upper and lower sides of the cell.

Convection heat transfer is considered on the walls of cell components. In order to simplify the simulation, Equation (7) is used to obtain the convective heat transfer coefficient [32].

$$h_h = 2.8 + 3.8u_w \left(\frac{W}{m^2 K} \right) \tag{7}$$

In Equation (7), u_w refers to the wind speed in m/s. Here, the speed of wind is considered as equal to 2 m/s in all of the simulations. In the present work, two coolants, water and SWCNT/water, are used. It should be noted that two volume fractions of the nanomaterials, 0.5% and 1%, are considered here. In order to determine density, specific heat, thermal conductivity and dynamic viscosity, the following equations are applied [33,34]:

$$\rho_{nf} = (1 - \varnothing)\rho_{bf} + \varnothing\rho_{np} \tag{8}$$

$$c_{nf} = (1 - \varnothing)c_{bf} + \varnothing c_{np} \tag{9}$$

$$k_{nf} = k_f \left(\frac{(1 - \varnothing) + 2\varnothing\left(\frac{k_{CNT}}{k_{CNT} - k_{bf}}\right) \ln\left(\frac{k_{CNT} + k_{bf}}{2k_{bf}}\right)}{(1 - \varnothing) + 2\varnothing\left(\frac{k_{bf}}{k_{CNT} - k_{bf}}\right) \ln\left(\frac{k_{CNT} + k_{bf}}{2k_{bf}}\right)} \right) \tag{10}$$

$$\frac{\mu_{nf}}{\mu_{bf}} = \frac{1}{(1 - \varnothing)^{2.5}} \tag{11}$$

where subscripts of *bf*, *nf* and *np* refer to base fluid, nanofluid and nano particle, respectively. In order to generate mesh, ANSYS Meshing is applied. To evaluate grid independency, different sizes were tested and the optimal condition is selected. In Figure 3, average temperature of the cell, in case of using water as coolant with mass flow rate of 0.003 kg/s, ambient temperature of 30 °C and solar radiation of 1000 W/m², with different numbers of elements, is shown. According to this figure, utilization of the model with around 2,400,000 mesh is the optimal condition and further reduction in the size does not affect the results. The meshed model in optimal condition is illustrated in Figure 4.
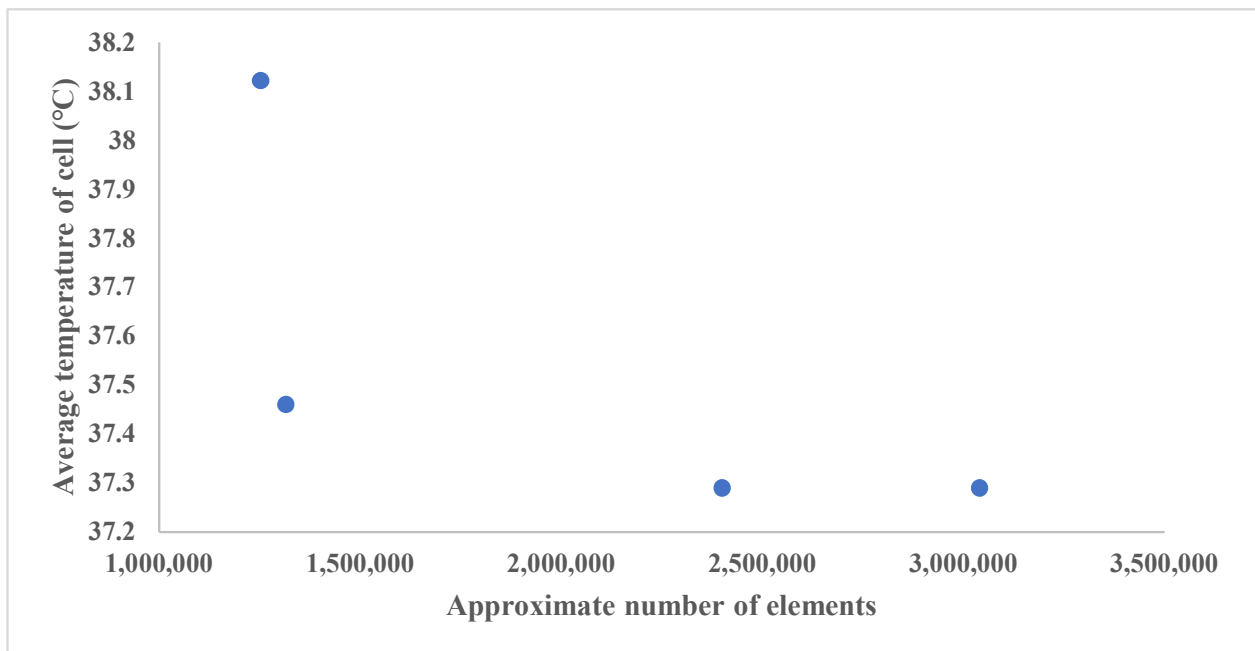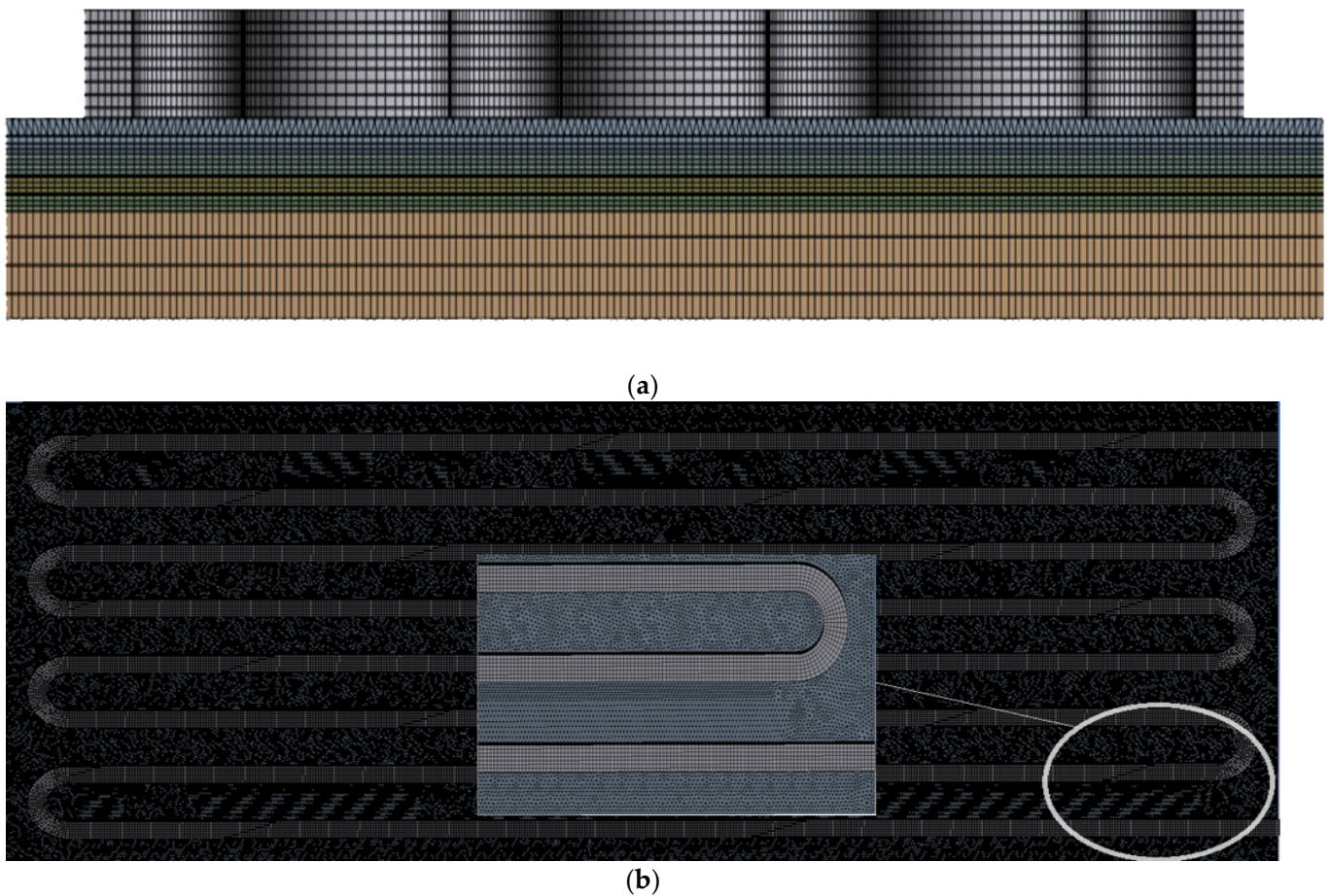

Figure 3. Variations in the average cell temperature vs. number of elements.

(a)

(b)

Figure 4. Meshed model in optimal element size: (**a**) 1st view (**b**) 2nd view.

Beside the energy analysis, exergy analysis is implemented on the system. The equations used for the exergy analysis are obtained from Ref. [35]. According to this reference, inlet exergy of the system, considering both coolant and the cell, is determined as follows:

$$\sum \dot{Ex}_{in} = \dot{Ex}_{in,th,PV} + \dot{Ex}_{in,el,PV} \tag{12}$$

where the first and second terms on the right hand side, thermal and electrical exergy, respectively, are determined as follows:

$$\dot{Ex}_{in,th,PV} = \dot{m}_f \cdot C_{pf} \cdot \left[(T_{av,i,PV} - T_0) - T_0 \cdot ln \frac{T_{av,i,PV}}{T_0} \right] \tag{13}$$

$$\dot{Ex}_{in,el,PV} = A_{PV} \cdot I \cdot \left[1 - \frac{4}{3} \left(\frac{T_a}{T_s} \right) + \frac{1}{3} \cdot \left(\frac{T_a}{T_s} \right)^4 \right] \tag{14}$$

where $\dot{m}_f$ is mass flow rate of the fluid, C_{pf} is the specific heat of the fluid, T_0 is the ambient temperature, T_s is sun surface temperature and is equal to 5777 K, A is solar cell area and I refers to the solar radiation. $T_{av,i,PV}$ is calcuated as follows:

$$T_{av,i,PV} = \frac{T_{fs} + T_{out,PV}}{2} \tag{15}$$

where T_{fs} is temperature of fluid supply and $T_{out,PV}$ is the outlet fluid temperature of PV module. Outlet exergy of the system is determined as follows:

$$\sum \dot{Ex}_{out} = \dot{Ex}_{out,th,PV} + \dot{Ex}_{out,el,PV} \tag{16}$$

The right hand side terms are calculated as follows:

$$\dot{Ex}_{out,th,PV} = \dot{m}_f \cdot C_{pf} \cdot \left[(T_{out,PV} - T_0) - T_0 \cdot ln \frac{T_{out,PV}}{T_0} \right] \tag{17}$$

$$\dot{Ex}_{out,el,PV} = A_{PV} \cdot \beta \cdot I \cdot \left[1 - \frac{4}{3} \left(\frac{T_a}{T_s} \right) + \frac{1}{3} \cdot \left(\frac{T_a}{T_s} \right)^4 \right] \tag{18}$$

The exergy efficiency of the system is determined as follows:

$$\eta_{ex} = \frac{\sum \dot{Ex}_{out}}{\sum \dot{Ex}_{in}} \tag{19}$$

In this study, firstly, a numerical simulation is implemented by considering different conditions including two mass flow rates of coolant, two concentrations of the nanofluids, two solar radiations and two ambient temperatures. Afterwards, based on the determined values for the generated electricity, efficiency of the cell and temperature at the outlet of the channel, the exergy analysis is carried. Results of the study are presented and discussed in the following section.

3. Results and Discussion

After preparing the modeling and grid independency evaluation, a comparison is performed between the results of the current simulation and a previous study by Birjandi et al. [31], in case of no cooling. As shown in Table 1, the obtained data are very close in the case of ambient temperature of 18 °C, q_s of 1000 W/m^2. According to the comparison, the results are very close to each other which validates the present model and simulation. Afterwards, simulation is performed by considering different working conditions. Two ambient temperatures, 30 and 40 °C, two solar radiations, 600 and 1000 W/m^2, three coolants, water and SWCNT/water in 0.5% and 1% concentrations, and two mass flow rates of coolants, 0.0015 and 0.003 kg/s, are considered in order to investigate different factors and their impacts on the cell average temperature and efficiency enhancement in comparison with the condition of no cooling.

Table 1. Comparison between the present and previous studies.

Wind Speed (m/s)	Average Temperature of the Current Simulation (°C)	Average Temperature in the Previous Work (Approximated) [31] (°C)
2	49.25	44.83
3	42.43	40.05
4	38.12	37.23

3.1. Energy Analysis

As the first analysis, the performance of the cell is determined based on its energy efficiency under various operating states. Using this cooling method causes reduction in the temperature of the cell. In Figure 5, temperature contour of the cell in case of ambient temperature of 40 °C and mass flow rate of 0.0030 kg/s, solar radiation of 600 W/m^2 using water as the coolant is illustrated.
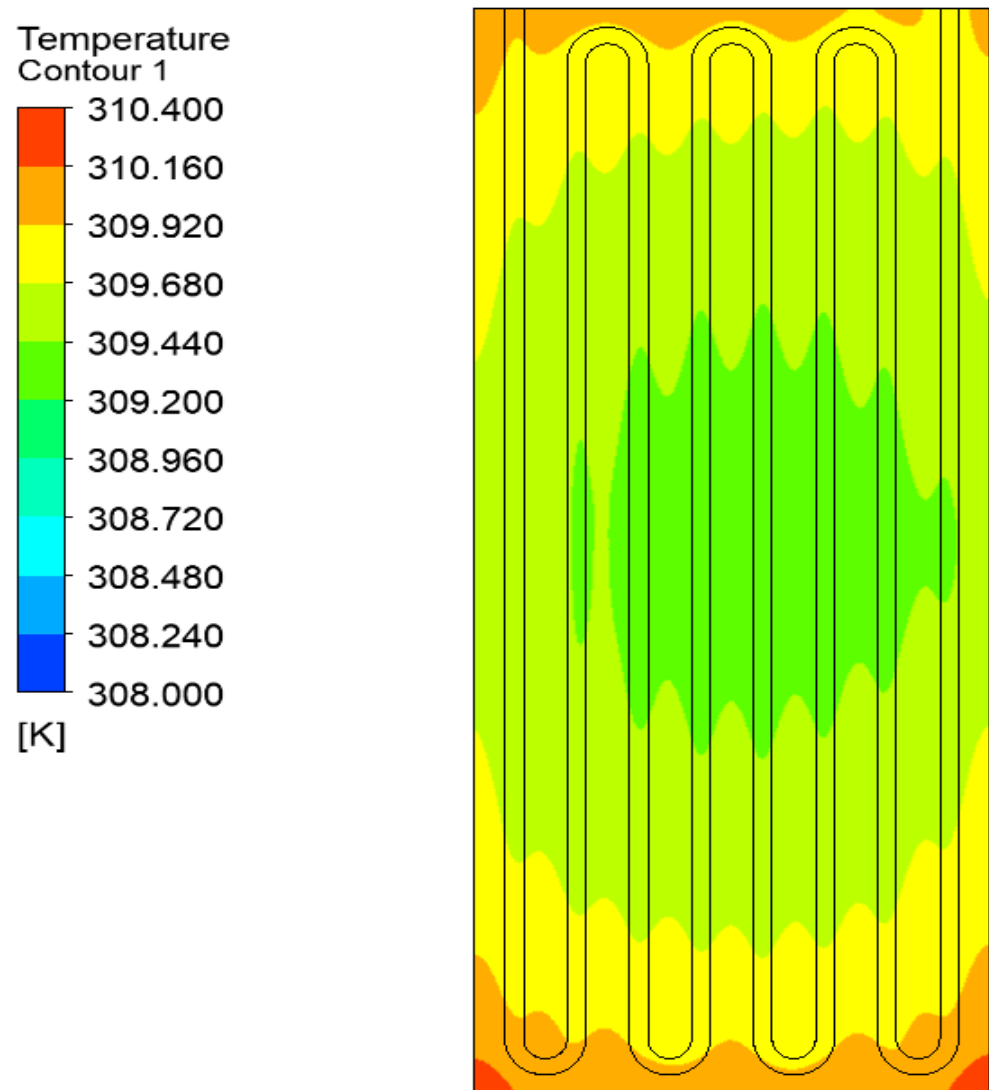
Figure 5. Cell temperature contour using water in mass flow rate of 0.0030 kg/s and ambient temperature of 40 °C.

3.2. Effect of Mass Flow Rate

In Figure 6, average temperature of the cell in different conditions, without any cooling, is presented. According to the determined values of temperature, the maximum temperature in condition of no cooling is around 68.09 °C for solar radiation of 1000 W/m^2 and ambient temperature of 40 °C. In Figure 7a–d, average temperatures of the cell in different conditions are presented. Average cell temperatures in condition of solar radiation of 1000 W/m^2 and ambient temperature of 40 °C are around 41.42 and 40.7 for water mass flow rates of 0.0015 kg/s and 0.0030 kg/s, respectively. It can be noticed that making use of water for thermal management causes remarkable decrement in the average temperature. Furthermore, it is concluded that increment in the mass flow rate of the coolants causes reduction in the average cell temperature, which means higher efficiency. With increment in the mass flow rate, the velocity of the fluid in constant area of the channel would be increased and, consequently, the Reynolds number is increased which causes higher convective heat transfer coefficient. Higher convective heat transfer coefficient means higher ability of heat removal from the cell, which means lower temperature and improved efficiency.
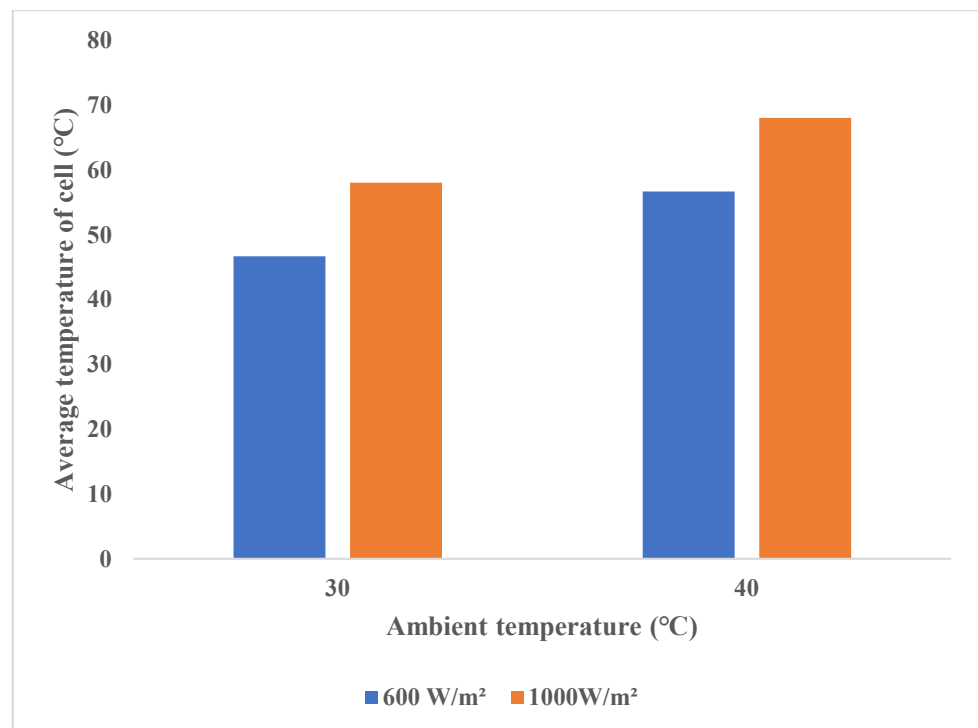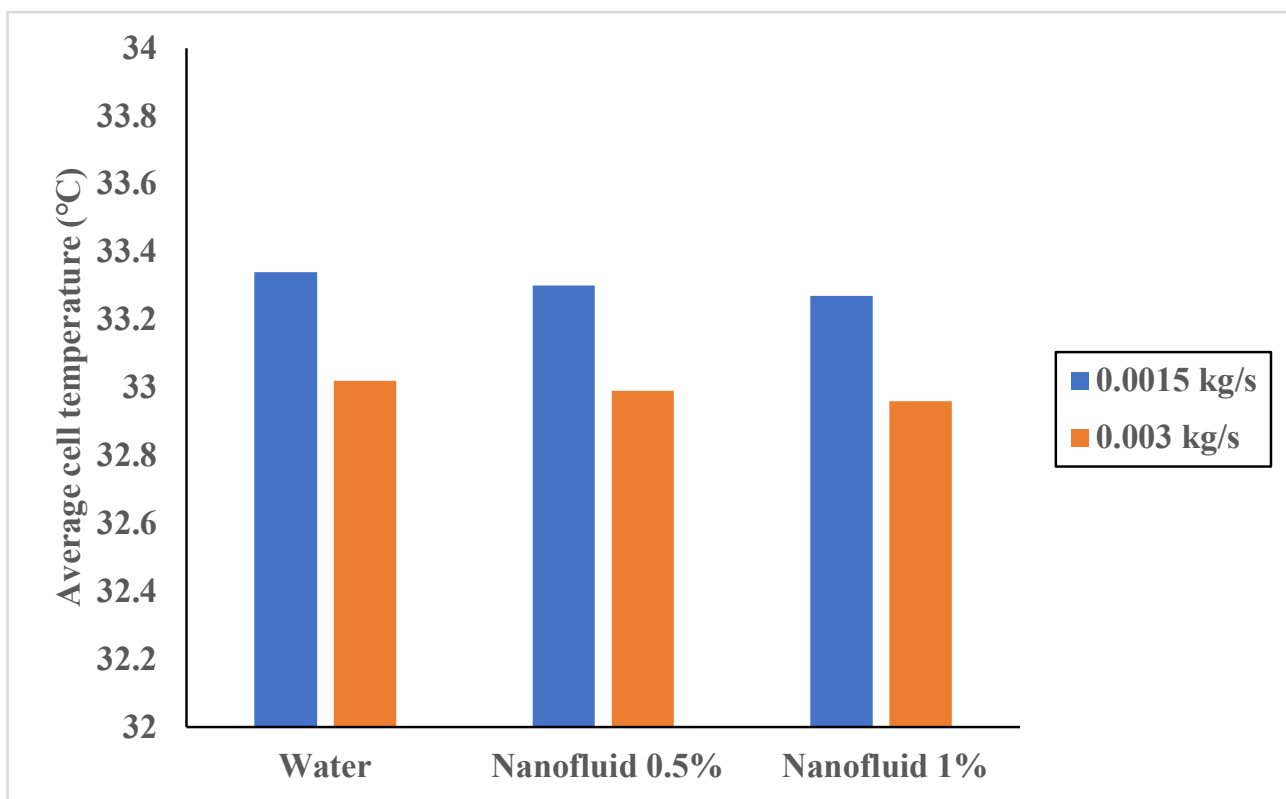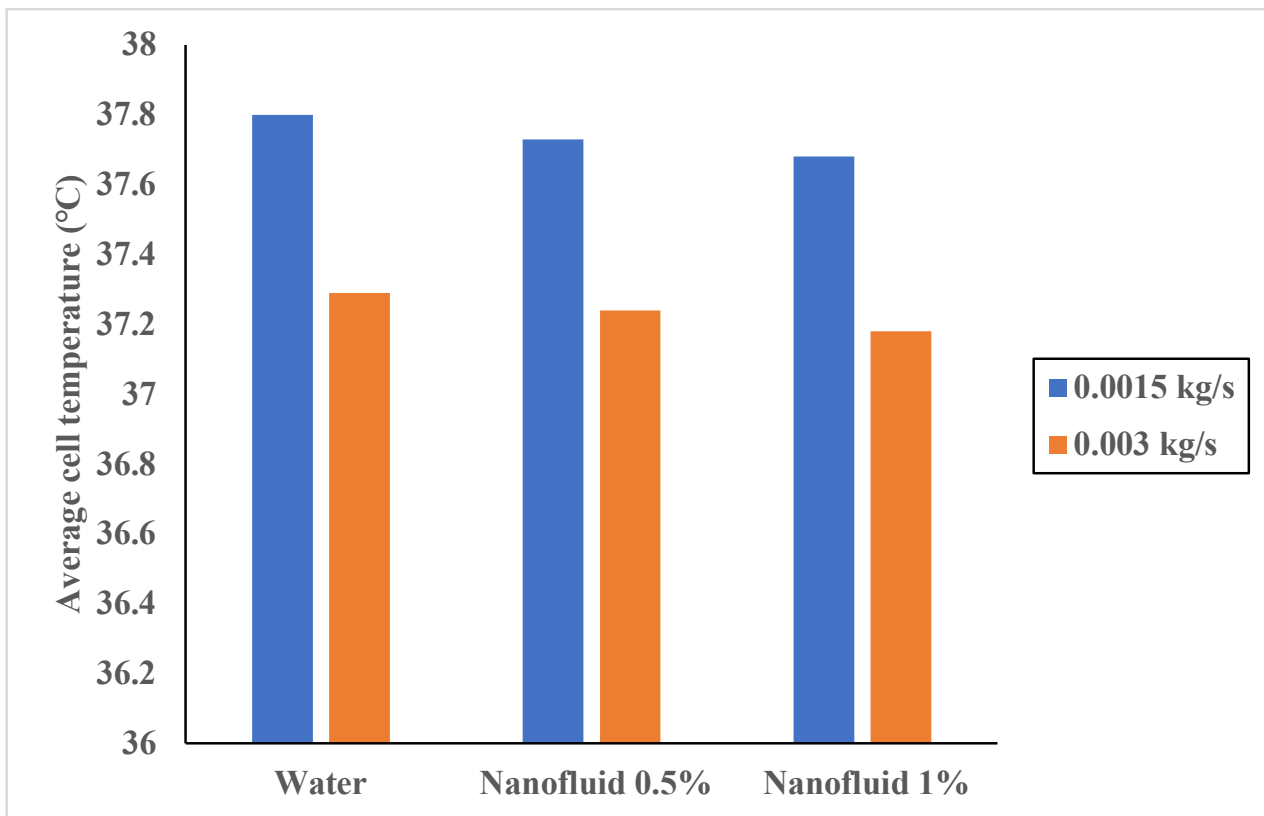
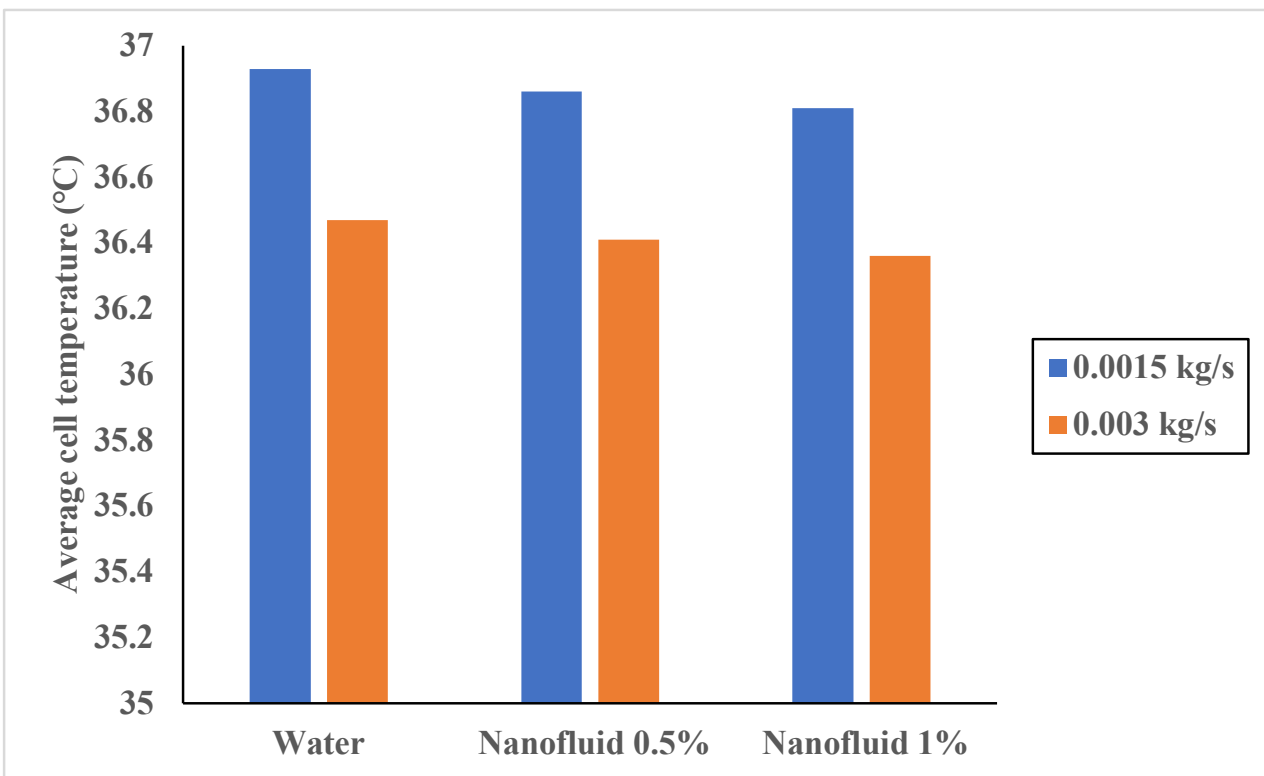**Figure 6.** Average temperature of the cell without cooling.
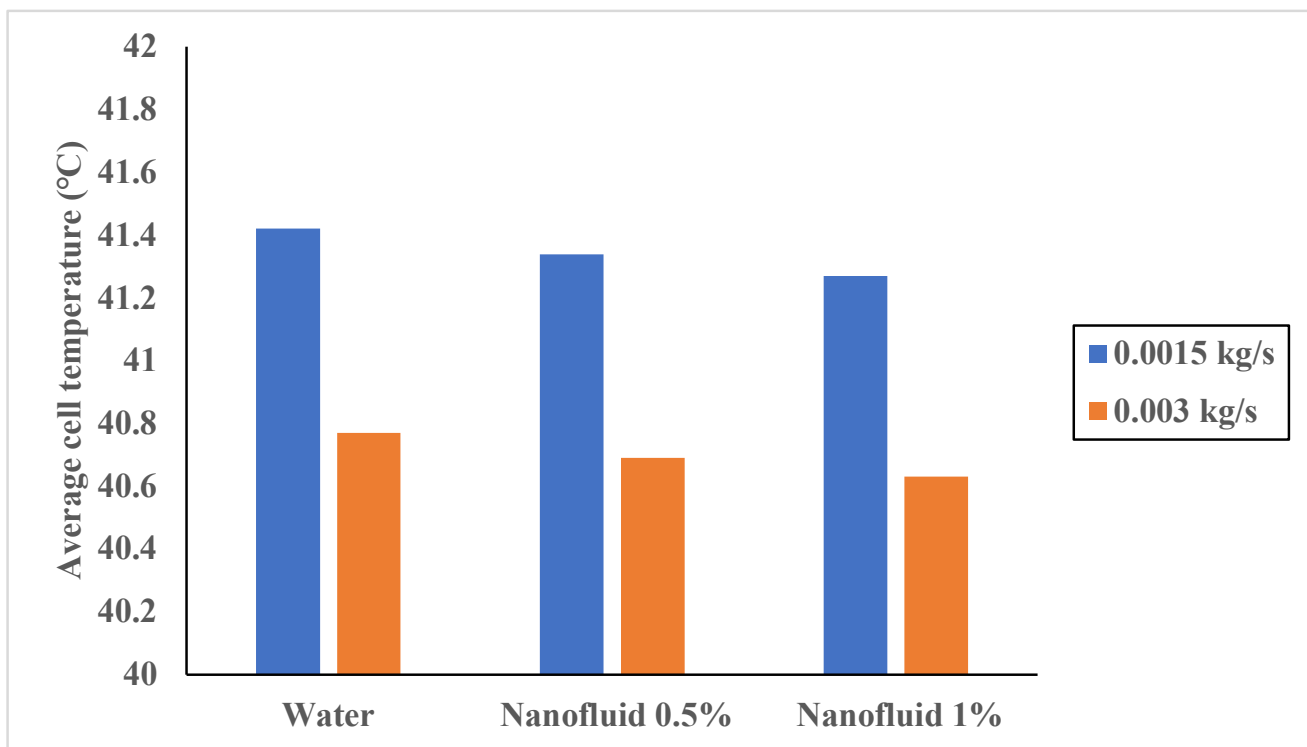

(**a**)

Figure 7. *Cont.*

(**b**)

(**c**)

Figure 7. *Cont.*

(d)

Figure 7. Average temperature of the cell for (**a**) solar radiation of 600 W/m^2 and ambient temperature of 30 °C, (**b**) solar radiation of 1000 W/m^2 and ambient temperature of 30 °C, (**c**) solar radiation of 600 W/m^2 and ambient temperature of 40 °C, and (**d**) solar radiation of 1000 W/m^2 and ambient temperature of 40 °C.

3.3. Effect of Concentration

As shown in Figure 7a–d, it can be noticed that using the nanofluid causes better cooling of the cell and lower temperature. As was denoted, dispersion of SWCNTs in water increases the thermal conductivity. By considering the same condition, i.e., equal Nusselt number, convective heat transfer coefficient would be increased regarding the higher thermal conductivity due to the existence of the conductive nanostructures. Further increment in the concentration of SWCNts causes further increase in the thermal conductivity. As a consequence, the convective heat transfer coefficient would be further increased which means more efficient thermal management and more decrement in the average cell temperature. It should be taken into account that there are some restrictions on increments in the concentration of solid phase. At high concentrations, the possibility of agglomeration of solid structures is increased that can deteriorate heat transfer. In addition, increase in concentration causes higher dynamic viscosity which would increase pressure loss and required power for circulating the fluid inside the cooling channels.

3.4. Effect of Ambient Temperature and Solar Radiation

Higher ambient temperature (Figure 7c,d) and solar radiation (Figure 7a–d) cause increment in the temperature of the cell without cooling. As shown in Figure 6, at solar radiation of 1000 W/m^2, an increase in ambient temperature from 30 °C to 40 °C causes an increment in average cell temperature from 58.09 °C to 68.09 °C. With increment in the ambient temperature, convective heat transfer to the surrounding is decreased while, in the case of 600 W/m^2 and ambient temperature of 40 °C, due to higher temperature of surrounding compared with the cooled cell, thermal energy is transferred to the cell. In addition, higher solar radiation means increment in the absorbed energy by the cell which

causes more increment in its internal energy and causes increase in temperature. In this case, applying thermal management would be more beneficial in term of efficiency enhancement. In case of solar radiation of 1000 W/m^2 and water mass flow rate of 0.0030 kg/s, increase in ambient temperature from 30 °C to 40 °C causes an increment in the average cell temperature from 36.47 °C to 40.77 °C. Although there is increment in the cell temperature due to increase in ambient temperature, its value is lower than in the case of no cooling. This is attributed to increment in heat transfer between the coolant and cell due to increase in temperature difference, which causes higher heat removal.

3.5. Performance Enhancement

To assess the effect of applied thermal management technique, efficiency of the cell must be compared with this condition. Use of cooling causes temperature reduction in the PV cell temperature and consequently the efficiency of the cell. In order to investigate its impact, performance enhancement as a new parameter (τ) is defined to assess the impact of cooling in different conditions. This parameter is defined as follows:

$$\tau = 100 * \frac{efficiency\ of\ the\ cell\ with\ cooling - efficiency\ of\ the\ cell\ without\ cooling}{efficiency\ of\ the\ cell\ without\ cooling}$$

Performance enhancement of the cell in different cooling modes is represented in Figure 8. It can be noticed that increase in the mass flow rate, solar radiation and concentration of the nanofluid causes higher efficiency enhancement which means improvement in the cooling of the cell. The maximum performance enhancement, for mass flow rate of 0.003 kg/s, solar radiation of 1000 W/m^2, nanofluid concentration of 1% and ambient temperature of 40 °C, is around 49.42%, which is remarkable and shows the effectiveness of this technique in significant enhancement of efficiency, while in cases of applying water as coolant the maximum value of performance enhancement is approximately 49.17%. This means that using the nanofluid in this range of concentration does not remarkably improve efficiency in comparison with water. The maximum improvement in the efficiency by using the proposed approach in this study is very significant. For instance, in the previous study [31], utilizing Multi Walled Carbon Nanotube (MWCNT)-Fe$_3$O$_4$/water with 0.3% concentration and mass flow rate of 0.00020 kg/s, the highest enhancement in efficiency compared with no cooling condition was around 35%.

(a)

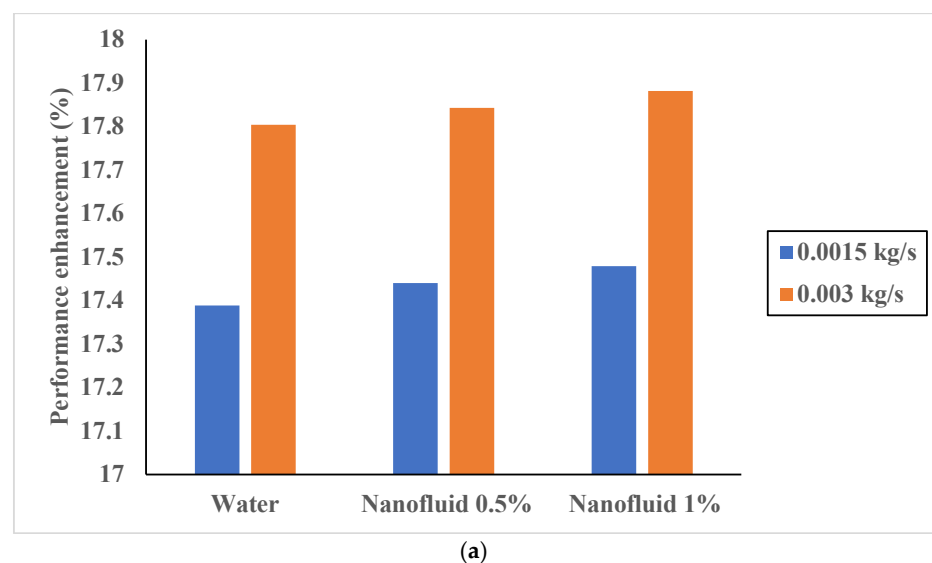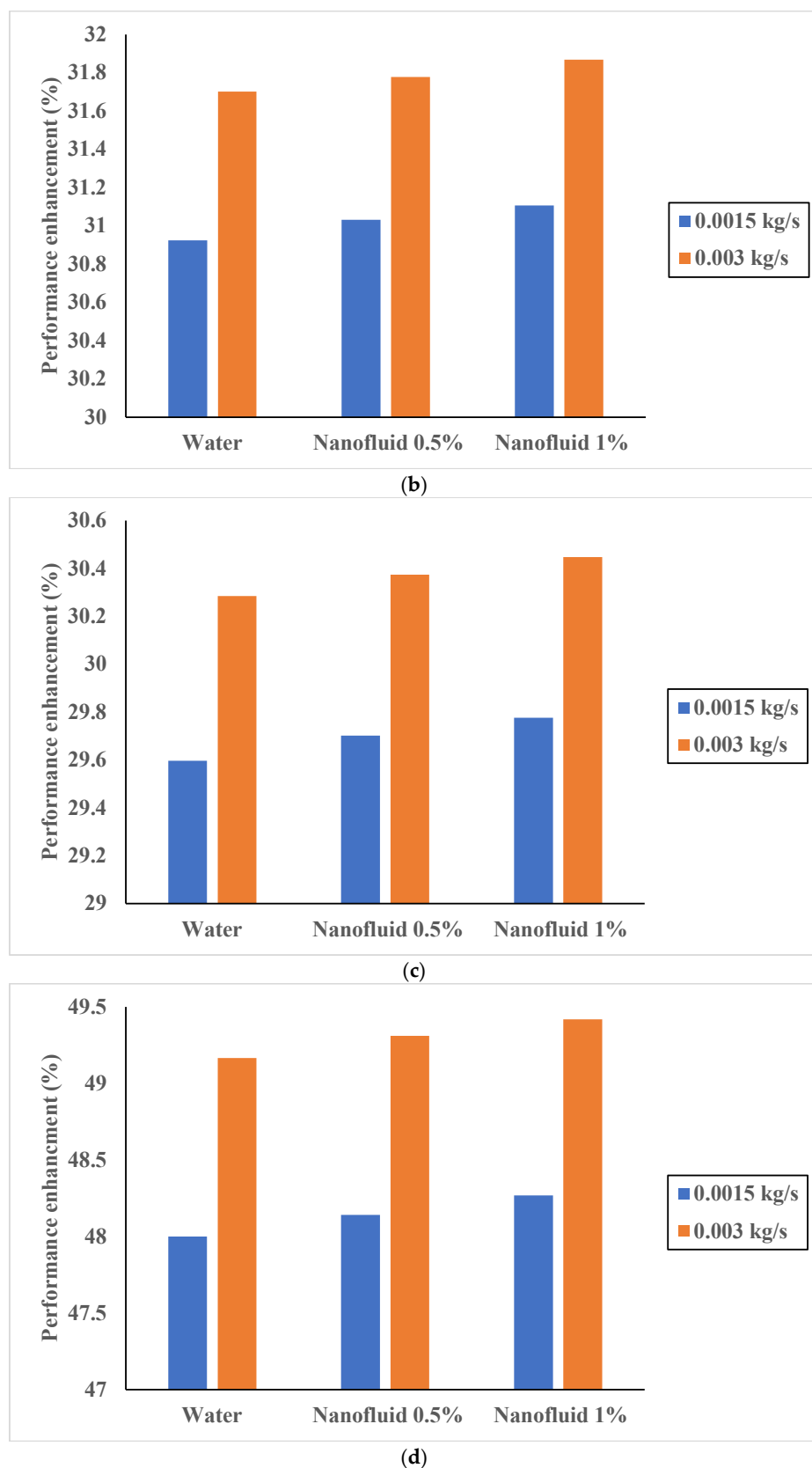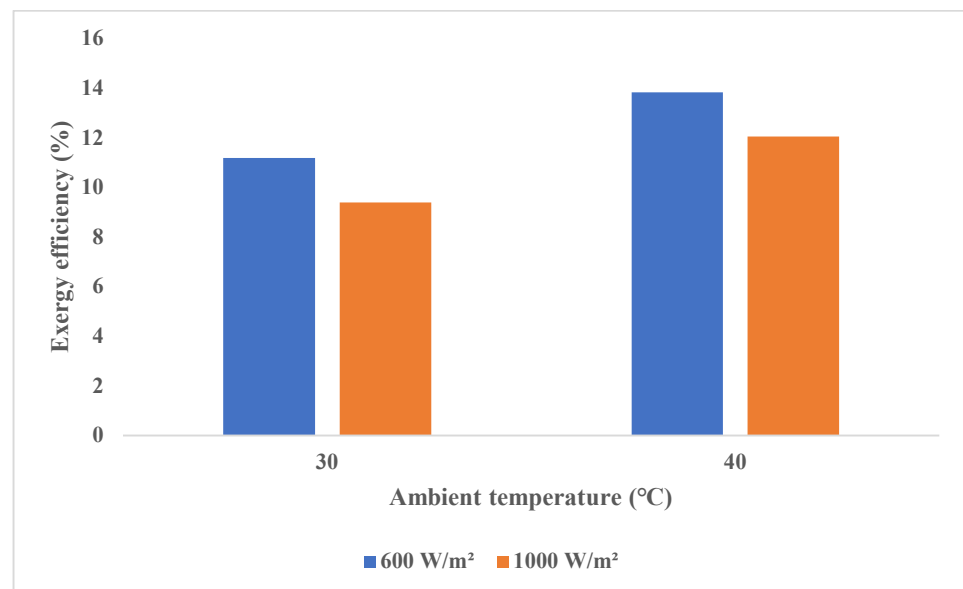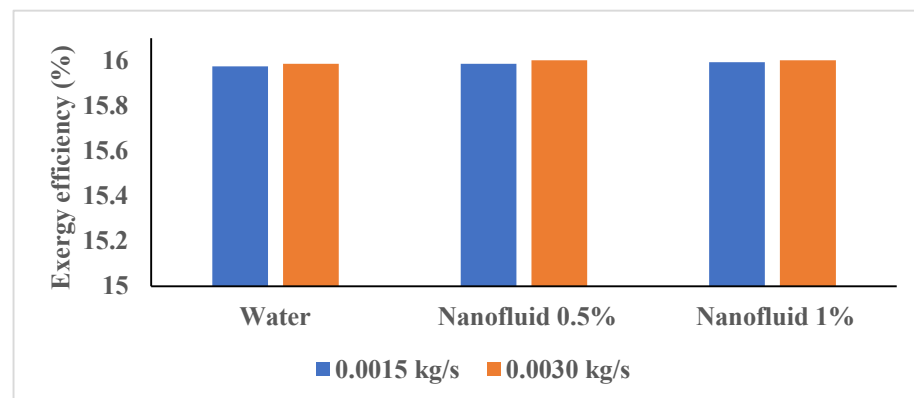**Figure 8.** *Cont.*

(b)

(c)

(d)

Figure 8. Performance enhancement of the cell for (**a**) solar radiation of 600 W/m^2 and ambient temperature of 30 °C, (**b**) solar radiation of 1000 W/m^2 and ambient temperature of 30 °C, (**c**) solar radiation of 600 W/m^2 and ambient temperature of 40 °C, and (**d**) solar radiation of 1000 W/m^2 and ambient temperature of 40 °C.

3.6. Exergy Analysis

Due to the energy absorption of the coolant in addition to the improvement in the electrical output of the cell, it is anticipated to show higher exergy efficiency in the case of using coolants. In Figure 9a–e, exergy efficiency of the system in different conditions is represented. It can be noticed that applying cooling (Figure 9b–e) can significantly improve exergy efficiency compared with no cooling (Figure 9a). Moreover, it is concluded that increment in both ambient temperature and solar radiation causes decrement in the overall exergy efficiency of the system which is attributed to the reduction in the cell electrical output. Furthermore, it is seen that, for cases of high ambient temperatures, the exergy efficiency of the systems with lower mass flow rate of coolant is higher, which is attributed to the higher thermal exergy of the system. According to the obtained data, it can be denoted that the maximum exergy efficiency of the cell is obtained in case of solar radiation of 600 W/m^2 and ambient temperature of 30 °C, which is around 15.987% and 16.002% for water and for the nanofluid with 1% concentration, respectively.

(**a**)

(**b**)

Figure 9. *Cont.*
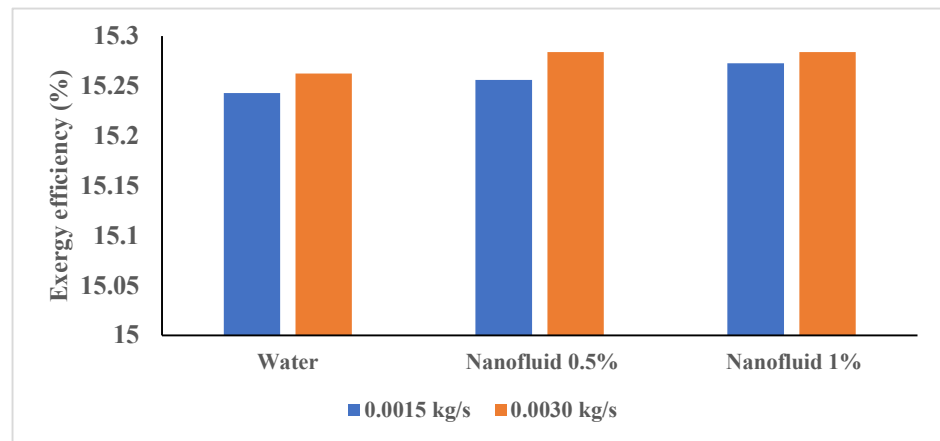
(**c**)
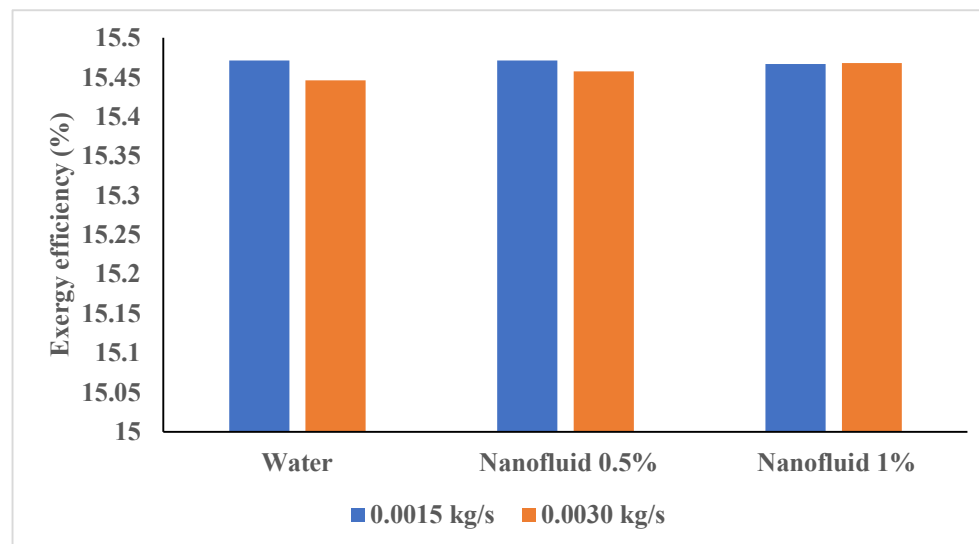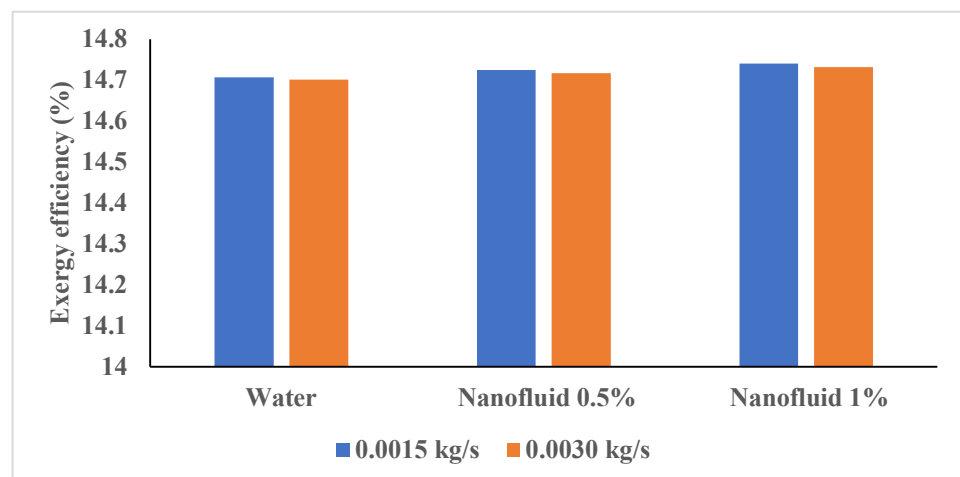

(**d**)

(**e**)

Figure 9. Exergy efficiency of the system for (**a**) without cooling (**b**) solar radiation of 600 W/m^2 and ambient temperature of 30 °C, (**c**) solar radiation of 1000 W/m^2 and ambient temperature of 30 °C, (**d**) solar radiation of 600 W/m^2 and ambient temperature of 40 °C, and (**e**) solar radiation of 1000 W/m^2 and ambient temperature of 40 °C.

4. Sensitivity Analysis

Despite the fact that all of the considered factors influence the efficiency enhancement of the cell, their impact is different and some are more effective. In order to evaluate impact of the variables, including ambient temperature, solar radiation and concentration of the nanofluid, sensitivity analysis must be carried out. This procedure is performed by determining dependency factor, which is in a range of −1 and 1. Higher absolute value of this parameter means higher influence of the corresponding variable. It should be noted that negative and positive values reveal decrement and increment in the output as the consequence of increment in the related variable. Relevancy factor of the parameters, by consideration of efficiency enhancement as the output, is determined by using Equation (12) as follows [36]:

$$r = \frac{\sum_{i=1}^{N} \left(X_{k,i} - \overline{X}_k \right) \left(y_i - \overline{y} \right)}{\sqrt{\sum_{i=1}^{N} \left(X_{k,i} - \overline{X}_k \right)^2 \sum_{i=1}^{N} \left(y_i - \overline{y} \right)^2}} \tag{20}$$

where $\overline{y}$ is average value of the output and y_i refers to the ith output value. $\overline{X}_k$ is the average value of the kth input variable and $X_{k,i}$ is the ith value of the kth input. Determined values for the variables are represented in Figure 10. It can be noticed that the relevancy factor value for solar radiation is the highest, followed by ambient temperature, mass flow rate of coolants and the concentration of nanofluid, respectively. It can be concluded that solar radiation has the highest influence on the variations of system efficiency; in another word, variations in this parameter change the efficiency more significantly compared with other considered factors. Moreover, it can be denoted that the effect of concentration, regarding its very low relevancy factor, is negligible compared with the three others.
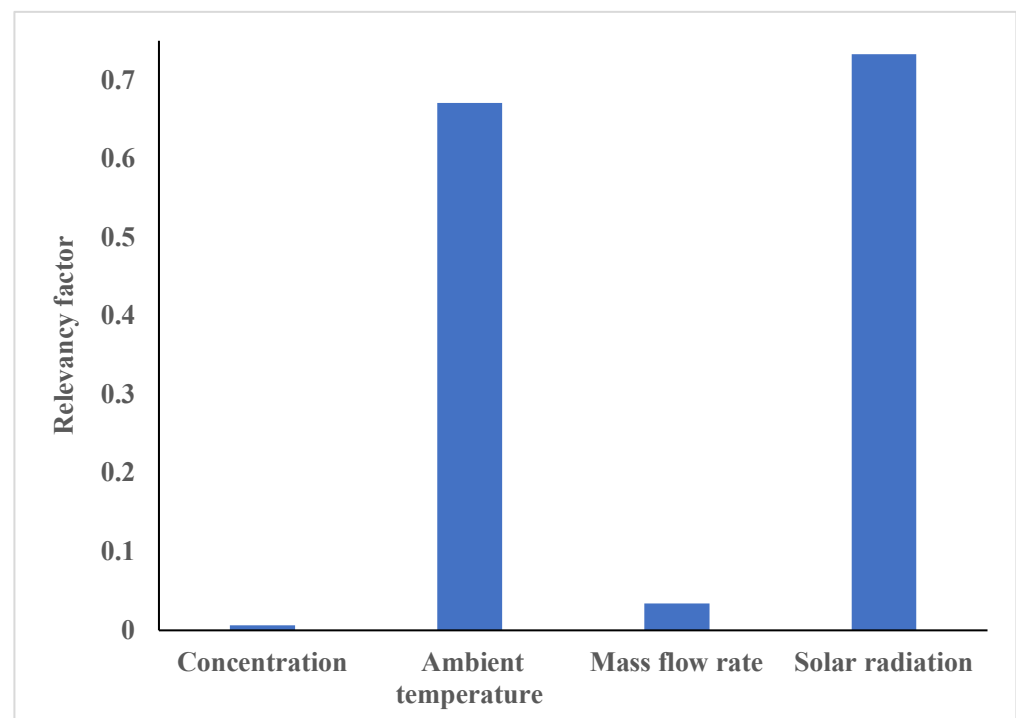
Figure 10. Values of relevancy factor for different parameters.

5. Conclusions

In the present article, effects of solar radiation, ambient temperature, mass flow rate of coolants and concentration of the nanofluid on the performance of solar cell are investigated. It is noticed that use of the nanofluids leads to further enhancement in performance enhancement of the cell efficiency; however, its impact is very low. The maximum enhancements in the cell efficiency in the present study by using the nanofluid, with concentration

of 1%, and water are around 49.42% and 49.17%, respectively. In addition, it is noticed that increment in mass flow rate and concentration of the nanofluid causes higher reduction in temperature and, consequently, further enhancement in efficiency. Moreover, it is concluded that using the cooling technique is more beneficial, in term of performance enhancement, at higher solar radiation and ambient temperature. The maximum exergy efficiency of the system in cases of using water and nanofluid was around 15.987% and 16.002%, respectively. It is found that, by increasing solar radiation and ambient temperature, exergy efficiency decreased. Finally, sensitivity analysis is carried out on the performance enhancement of the cell when using the present cooling technique in order to assess the impacts of different parameters. The determined values of relevancy factors reveal that solar radiation has the highest impact, followed by ambient temperature, mass flow rate of the coolant and concentration of the nanofluid, respectively.

Author Contributions: Investigation, M.H.A. and F.M.M.; Methodology, M.S., M.H.A. and J.R.; Supervision, J.R.; Writing—Original draft, M.S.; Writing—Review & editing, M.H.A., J.R. and F.M.M. All authors have read and agreed to the published version of the manuscript.

Institutional Review Board Statement: Not applicable.

Informed Consent Statement: Not applicable.

Data Availability Statement: Not applicable.

Nomenclature

A	Area
C	Specific heat (J/kg.K)
Ex	Exergy (J)
k	Thermal conductivity (W/m.K)
r	Relevancy factor
T	Temperature (K)
μ	Viscosity (N/m.s)
ρ	Density (Kg/m^3)
$\varnothing$	Volume fraction
β	Cell efficiency
τ	Performance enhancement (%)
σ_{sb}	Stephan Boltzmann constant (W/m^2·K^4)
Subscripts	
a	Ambient
el	Electrical
h	Convection
in	Inlet
nf	Nanofluid
out	Outlet
pf	Pure fluid
rad	Radiation
S	Surface
w	Wind

References

1.　Amin, T.E.; Roghayeh, G.; Fatemeh, R.; Fatollah, P. Evaluation of Nanoparticle Shape Effect on a Nanofluid Based Flat-Plate Solar Collector Efficiency. *Energy Explor. Exploit.* **2015**, *33*, 659–676. [CrossRef]
2.　Wang, Y.; Kamari, M.L.; Haghighat, S.; Ngo, P.T.T. Electrical and thermal analyses of solar PV module by considering realistic working conditions. *J. Therm. Anal. Calorim.* **2020**, *144*, 1925–1934. [CrossRef]
3.　Daghigh, R.; Shahidian, R.; Oramipoor, H. A multistate investigation of a solar dryer coupled with photovoltaic thermal collector and evacuated tube collector. *Sol. Energy* **2020**, *199*, 694–703. [CrossRef]

4. El Haj Assad, M.; Alhuyi Nazari, M.; Rosen, M.A. Applications of renewable energy sources. In *Design and Performance Optimization of Renewable Energy Systems*; Academic Press: Cambridge, MA, USA, 2021; pp. 1–15.

5. Cai, W.; Li, X.; Maleki, A.; Pourfayaz, F.; Rosen, M.A.; Nazari, M.A.; Bui, D.T. Optimal sizing and location based on economic parameters for an off-grid application of a hybrid system with photovoltaic, battery and diesel technology. *Energy* **2020**, *201*, 117480. [CrossRef]

6. Zhang, W.; Maleki, A.; Rosen, M.A. A heuristic-based approach for optimizing a small independent solar and wind hybrid power scheme incorporating load forecasting. *J. Clean. Prod.* **2019**, *241*, 117920. [CrossRef]

7. Alhuyi Nazari, M.; Salem, M.; Mahariq, I.; Younes, K.; Maqableh, B.B. Utilization of Data-Driven Methods in Solar Desalination Systems: A Comprehensive Review. *Front. Energy Res.* **2021**, *9*, 742615. [CrossRef]

8. Wang, C.; Nehrir, M.H. Power management of a stand-alone wind/photovoltaic/fuel cell energy system. *IEEE Trans. Energy Convers.* **2008**, *23*, 957–967. [CrossRef]

9. Hasan, A.; Sarwar, J.; Shah, A.H. Concentrated photovoltaic: A review of thermal aspects, challenges and opportunities. *Renew. Sustain. Energy Rev.* **2018**, *94*, 835–852. [CrossRef]

10. Yunus Khan, T.M.; Soudagar, M.E.M.; Kanchan, M.; Afzal, A.; Banapurmath, N.R.; Akram, N.; Mane, S.D.; Shahapurkar, K. Optimum location and influence of tilt angle on performance of solar PV panels. *J. Therm. Anal. Calorim.* **2019**, *141*, 511–532. [CrossRef]

11. Maleki, A.; Ngo, P.T.T.; Shahrestani, M.I. Energy and exergy analysis of a PV module cooled by an active cooling approach. *J. Therm. Anal. Calorim.* **2020**, *141*, 2475–2485. [CrossRef]

12. Fouad, M.M.; Shihata, L.A.; Morgan, E.I. An integrated review of factors influencing the perfomance of photovoltaic panels. *Renew. Sustain. Energy Rev.* **2017**, *80*, 1499–1511. [CrossRef]

13. Mert, B.D.; Ekinci, F.; Demirdelen, T. Effect of partial shading conditions on off-grid solar PV/Hydrogen production in high solar energy index regions. *Int. J. Hydrogen Energy* **2019**, *44*, 27713–27725. [CrossRef]

14. Brinkworth, B. Estimation of flow and heat transfer for the design of PV cooling ducts. *Sol. Energy* **2000**, *69*, 413–420. [CrossRef]

15. Bahaidarah, H.M.S.; Baloch, A.A.B.; Gandhidasan, P. Uniform cooling of photovoltaic panels: A review. *Renew. Sustain. Energy Rev.* **2016**, *57*, 1520–1544. [CrossRef]

16. Sharma, S.; Micheli, L.; Chang, W.; Tahir, A.; Reddy, K.; Mallick, T. Nano-enhanced Phase Change Material for thermal management of BICPV. *Appl. Energy* **2017**, *208*, 719–733. [CrossRef]

17. Idoko, L.; Anaya-Lara, O.; McDonald, A. Enhancing PV modules efficiency and power output using multi-concept cooling technique. *Energy Rep.* **2018**, *4*, 357–369. [CrossRef]

18. Alizadeh, H.; Ghasempour, R.; Razi Astaraei, F.; Alhuyi Nazari, M. Numerical Modeling of PV Cooling by Using Pulsating Heat Pipe. In Proceedings of the 3rd International Conference and Exhibition on Solar Energy ICESE-2016, Tehran, Iran, 5–6 September 2016.

19. Ramkiran, B.; Sundarabalan, C.K.; Sudhakar, K. Sustainable passive cooling strategy for PV module: A comparative analysis. *Case Stud. Therm. Eng.* **2021**, *27*, 101317.

20. Shalaby, S.M.; Elfakharany, M.K.; Moharram, B.M.; Abosheiasha, H. Experimental study on the performance of PV with water cooling. *Energy Rep.* **2022**, *8*, 957–961. [CrossRef]

21. Ali, H.M. Recent advancements in PV cooling and efficiency enhancement integrating phase change materials based systems—A comprehensive review. *Sol. Energy* **2020**, *197*, 163–198. [CrossRef]

22. Rashidi, M.M.; Nazari, M.A.; Mahariq, I.; Assad, M.E.H.; Ali, M.E.; Almuzaiqer, R.; Nuhait, A.; Murshid, N. Thermophysical Properties of Hybrid Nanofluids and the Proposed Models: An Updated Comprehensive Study. *Nanomaterials* **2021**, *11*, 3084. [CrossRef]

23. Rashidi, M.M.; Alhuyi Nazari, M.; Mahariq, I.; Ali, N. Modeling and Sensitivity Analysis of Thermal Conductivity of Ethylene Glycol-Water Based Nanofluids with Alumina Nanoparticles. *Exp. Tech.* **2022**, 1–8. [CrossRef]

24. Ahmadi, M.H.; Mirlohi, A.; Nazari, M.A.; Ghasempour, R. A review of thermal conductivity of various nanofluids. *J. Mol. Liq.* **2018**, *265*, 181–188. [CrossRef]

25. KAbu-Nab, A.; Selima, E.S.; Morad, A.M. Theoretical investigation of a single vapor bubble during Al_2O_3/H_2O nanofluids in power-law fluid affected by a variable surface tension. *Phys. Scr.* **2021**, *96*, 035222. [CrossRef]

26. Morad, A.M.; Selima, E.S.; Abu-Nab, A.K. Thermophysical bubble dynamics in N-dimensional Al_2O_3/H_2O nanofluid between two-phase turbulent flow. *Case Stud. Therm. Eng.* **2021**, *28*, 101527. [CrossRef]

27. Ahmadi, M.H.; Ghazvini, M.; Sadeghzadeh, M.; Alhuyi Nazari, M.; Ghalandari, M. Utilization of hybrid nanofluids in solar energy applications: A review. *Nano-Struct. Nano-Objects* **2019**, *20*, 100386. [CrossRef]

28. Nazari, S.; Najafzadeh, M.; Daghigh, R. Techno-economic estimation of a non-cover box solar still with thermoelectric and antiseptic nanofluid using machine learning models. *Appl. Therm. Eng.* **2022**, *212*, 118584. [CrossRef]

29. Nazari, S.; Safarzadeh, H.; Bahiraei, M. Performance improvement of a single slope solar still by employing thermoelectric cooling channel and copper oxide nanofluid: An experimental study. *J. Clean. Prod.* **2019**, *208*, 1041–1052. [CrossRef]

30. Sadeghi, G.; Safarzadeh, H.; Ameri, M. Experimental and numerical investigations on performance of evacuated tube solar collectors with parabolic concentrator, applying synthesized Cu_2O/distilled water nanofluid. *Energy Sustain. Dev.* **2019**, *48*, 88–106. [CrossRef]

31.   Komeili Birjandi, A.; Eftekhari Yazdi, M.; Dinarvand, S.; Salehi, G.R.; Tehrani, P. Effect of Using Hybrid Nanofluid in Thermal Management of Photovoltaic Panel in Hot Climates. *Int. J. Photoenergy* **2021**, *2021*, 3167856. [CrossRef]

32.   Alizadeh, H.; Ghasempour, R.; Shafii, M.B.; Ahmadi, M.H.; Yan, W.-M.; Nazari, M.A. Numerical simulation of PV cooling by using single turn pulsating heat pipe. *Int. J. Heat Mass Transf.* **2018**, *127*, 203–208. [CrossRef]

33.   Aramesh, M.; Pourfayaz, F.; Kasaeian, A. Numerical investigation of the nanofluid effects on the heat extraction process of solar ponds in the transient step. *Sol. Energy* **2017**, *157*, 869–879. [CrossRef]

34.   Reddy, Y.R.O.; Reddy, M.S.; Reddy, P.S. MHD boundary layer flow of SWCNT-water and MWCNT-water nanofluid over a vertical cone with heat generation/absorption. *Heat Transf.—Asian Res.* **2019**, *48*, 539–555. [CrossRef]

35.   Ceylan, I.; Gürel, A.E. Exergetic analysis of a new design photovoltaic and thermal (PV/T) System. *Environ. Prog. Sustain. Energy* **2015**, *34*, 1249–1253. [CrossRef]

36.   Baghban, A.; Kahani, M.; Nazari, M.A.; Ahmadi, M.H.; Yan, W.-M. Sensitivity analysis and application of machine learning methods to predict the heat transfer performance of CNT/water nanofluid flows through coils. *Int. J. Heat Mass Transf.* **2019**, *128*, 825–835. [CrossRef]